J. Fluid Mech. (1969), *vol.* 37, *part* 2, *pp.* 307–323
Printed in Great Britain

Axisymmetric inertial oscillations of a fluid in a rotating spherical container

By KEITH D. ALDRIDGE† AND ALAR TOOMRE
Massachusetts Institute of Technology, Cambridge, Massachusetts

(Received 22 August 1968)

This paper describes an experiment performed with a fluid-filled sphere whose rotation speed about a fixed axis was forcibly varied in a slight but sinusoidal manner about a non-zero mean value. The object of this experiment was both to excite axisymmetric inertial eigen-oscillations within the relatively low viscosity fluid through the mild pumping action of the oscillatory Ekman boundary layer near the wall, and to measure and compare with theory some of the properties of such modes.

Seven distinct fluid resonances were detected via pressure measurements made along the axis for various ratios of the excitation to the mean rotation frequency. For the three most pronounced of those modes, the observed frequency ratios agree within $\frac{1}{2}$ of 1% with the corresponding ratios predicted from linear, small viscosity theory. The response amplitudes at the various resonances and the rates of decay upon switching off the excitation also compare favourably with theory, although the observed amplitudes are systematically lower and the decays more rapid by a few per cent to several tens of per cent.

The theory referred to above is largely that of Greenspan (1964, 1968). It is in part rederived here from energy considerations.

1. Introduction

The term 'inertial oscillations' has come to denote those oscillatory motions of a *rotating* fluid that owe their existence neither to free surfaces, nor to compressibility, nor to any density stratification. The present paper reports the excitation of some discrete eigenmodes of this kind within a spherical cavity. In a sense this is but an extension to a different geometry of the experiments of Fultz (1959), which themselves belong to a line of investigations dating back at least to Bjerknes & Solberg (1929) and to Kelvin (1880). Fultz excited similar inertial modes within a right circular cylinder by means of a small disk immersed in the fluid and oscillated up and down along the cylinder (and rotation) axis at various constant frequencies. Besides its geometry, however, our study differs also in its special emphasis on ascertaining the effects of a small but finite viscosity. In addition, our method of exciting these fluid oscillations should itself be of some interest.

† Now at the Meteorological Office, Bracknell, Berkshire, England.

That method was suggested by the following analogy: Imagine a small-amplitude gravity wave in a relatively shallow, non-rotating basin of fluid. In the presence of a slight viscosity, the amplitude of this wave will decay with time, if for no other reason than the energy dissipation in the boundary layer near the rigid bottom. Note, however, that that decay will not require viscous diffusion upwards through the full depth of the fluid. Rather, the slight vertical secondary flow from the spatially and time-dependent bottom boundary layer will phase itself so as to drain wave energy from the bulk of the fluid through the action of pressure forces alone.

The above implies that if this phase relation to the rest of the oscillation were modified sufficiently, one could actually *excite* or amplify waves in that basin. For instance, suppose the bottom were made of a (one-dimensionally) flexible material that could be forced to slide back and forth in its own plane with a speed harmonically dependent both on time and on the horizontal co-ordinate in the direction of movement. Then an appreciable standing wave would indeed be built up, provided the excitation frequency were chosen to approximate the inviscid natural frequency of a wave of the same length as the prescribed sliding. Even precisely at resonance, however, such a fluid response would not blow up with vanishing viscosity; on the contrary, that steady-state amplitude would be virtually independent of the viscosity.

In the experiment we are about to describe, it was the externally driven oscillation of the sphere about its axis of mean rotation that corresponded to the sliding bottom. Because its tangential speed and also the properties of the boundary layer itself depended on the latitude, it was unnecessary to make this container flexible. In fact, unlike the spatially sinusoidal forcing described above, the pumping through the time-dependent Ekman boundary layers here proved significantly non-orthogonal to a number of different modes of fluid oscillation. It was therefore possible to 'tune in' to any particular mode simply by choosing an appropriate *ratio* of the frequency of reciprocation and the mean speed of rotation.

2. Experimental arrangements

Our apparatus consisted primarily of a polished, transparent sphere of internal radius $a = 10$ cm, with discrepancies between its various diameters not exceeding 0·2%. This sphere, completely filled with water as the usual working fluid, was fastened to a shaft that was in turn supported vertically by bearings mounted on a turntable. By means of a crank and torsion-bar arrangement, the shaft and sphere together could be made to reciprocate relative to the turntable with an arbitrary half-amplitude ϵ and a frequency ω. The turntable itself was driven coaxially with the shaft at a steady rate Ω, thereby imparting to the sphere the instantaneous angular speed

$$\Omega_s(t) \cong \Omega + \epsilon\omega \cos \omega t. \tag{1}$$

For technical reasons, the frequency of oscillation was always kept constant at $\omega \cong 6{\cdot}2$ rad/sec. Desired changes in the ratio ω/Ω between successive observations

were brought about by altering the turntable speed via a continuously variable transmission.

Various resonant oscillations of the fluid in the cavity were made visible by introducing dye and also with suspended aluminium flakes. They were in addition measured crudely with a manometer tube extending to the centre of the sphere and filled with alcohol to raise the meniscus above the top of the sphere for easier viewing. All the amplitude and phase measurements reported below, however, refer to disturbance pressure differences between the tip of a non-rotating, 2 mm o.d. hollow tube immersed along the axis usually to the centre of the sphere, and the free surface of the fluid at a 1·2 cm diameter hole drilled into the 'north pole' of the container.

The said probe was connected through stiff tubing to an inductive differential pressure transducer, the other port of which remained open to the atmosphere. The electrical output of this transducer and simultaneous data concerning the phase of the mechanical oscillation were transmitted to a multi-channel chart recorder. The dynamical response of the probe-transducer-recorder combination was frequently calibrated with respect both to amplitude and phase by immersing the probe tip in a beaker of water that was shaken vertically at 1 c/s with appropriate optically measured amplitudes of the order of 1 mm. The mean rotation speed Ω, and even the oscillation half-amplitude ϵ of the sphere while the turntable was *in motion*, was determined with an electronic stopwatch. Numerous other probe calibrations, averagings of data, and refinements of apparatus were undertaken to ensure that any errors in the reported pressure coefficients remained of the order of 1 or 2% of the maximum observed values to be quoted below.

3. Theoretical discussion

For obvious reasons of symmetry, only those axisymmetric fluid oscillations which involve no motions across the equatorial plane of the sphere could be excited in the present experiment. Even with this restriction, however, the number of eligible *inviscid* and supposedly infinitesimal eigen-modes was known to be denumerably infinite. The eigen-frequencies of such modes were predicted by Stewartson & Roberts (1963, equation (5.10)) to be

$$\omega_{nm} = 2\Omega x_{nm}, \tag{2}$$

where x_{nm} is the mth of the n zeroes of the first associated Legendre function $P^1_{2n+2}(x)$ in the range $0 < x < 1$, here labelled in ascending order.

The velocity components of the (n, m)th of these modes in the natural cylindrical polar co-ordinates r, ϕ, z may be written

$$(u_r, u_\phi, u_z) = \epsilon\omega_{nm} a \,\mathrm{Re}\{A_{nm} \exp(i\omega_{nm} t)(iU, -U/x_{nm}, iW)\}, \tag{3}$$

where

$$U(R,Z) = \frac{1}{R}\frac{\partial\psi_{nm}}{\partial Z}, \quad W(R,Z) = -\frac{1}{R}\frac{\partial\psi_{nm}}{\partial R}, \tag{4}$$

and the stream function

$$\psi_{nm}(R,Z) = R^2 Z \prod_{k=1}^{n} \left(1 - \frac{1-x_{nm}^2}{1-x_{nk}^2} R^2 - \frac{x_{nm}^2}{x_{nk}^2} Z^2\right). \tag{5}$$

Here also $R = r/a$ and $Z = z/a$ for brevity, and the complex constant A_{nm} is a dimensionless amplitude. This product representation of the inviscid eigen-modes complements Greenspan's (1964) Legendre function expression (3.45) for the spatial part of the disturbance pressure.

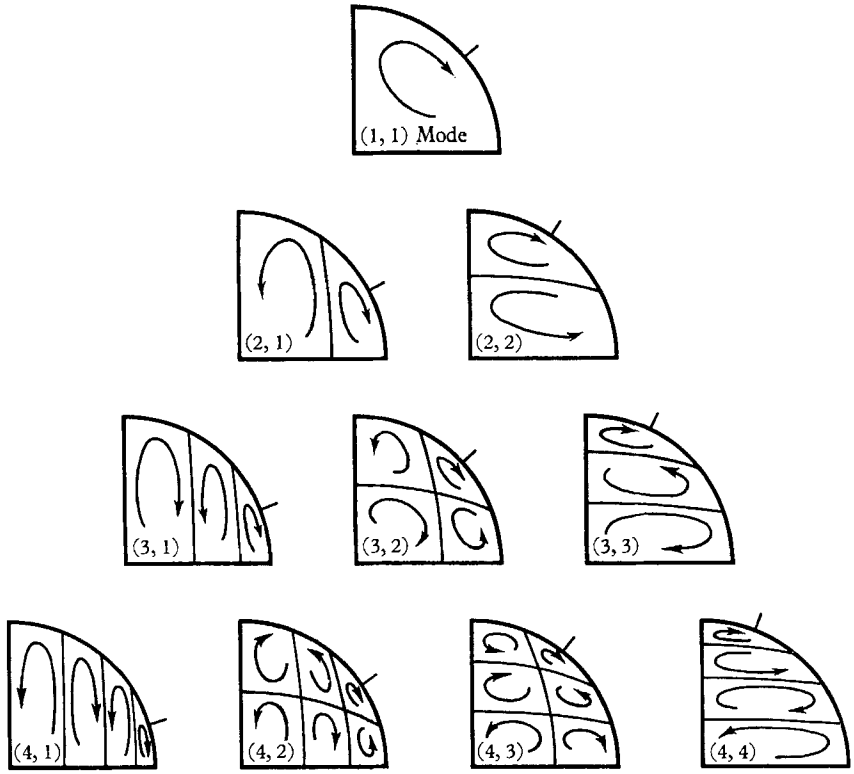

FIGURE 1. Identification chart. Drawn to scale are the loci where $\psi = 0$; the critical latitudes are also marked. The rotation axis is vertical.

Because of the $k = m$ factor in equation (5), the stream function ψ_{nm} quite properly vanishes on the sphere $R^2 + Z^2 = 1$. In addition, that equation prescribes exactly $(n-1)$ other elliptical cell boundaries along which $\psi_{nm} = 0$ in any meridional plane. It is easily seen that the semi-major and minor axes of those ellipses are always greater and smaller than a, respectively. (A less obvious property of those ellipses is that they are all tangent to the rhombus

$$(1-x_{nm}^2)^{\frac{1}{2}} |R| + x_{nm} |Z| = 1.)$$

Figure 1 displays the nodal surfaces of the first four families of eigen-modes thus deduced from equation (5).

The excitation, decay and superposition of the *viscous* counterparts to these modes in our experiment constitutes a more difficult theoretical problem. In a

strict sense that problem has not yet been solved even in the combined limit of infinitesimal amplitude and of vanishing viscosity. However, probably the best approximation to such a comprehensive theory is that of Greenspan (1964), especially §6; see also §§2.13 and 2.14 of Greenspan (1968). It appears to leave unsettled only the non-uniformities arising from the fact that, no matter how small the viscosity, there are (i) neighbourhoods of certain critical latitudes, and (ii) modes of sufficiently high order n which require a fuller analysis.

Our remaining theoretical remarks do not even presume to resolve those possibly academic difficulties. They are meant instead to supplement Greenspan's own accounts with certain more explicit formulae and with some needed physical interpretation.

This discussion simply postulates that, just as in the wave tank example, all *direct* effects of a slight kinematic viscosity ν on at least the low-order modes should be confined to thin boundary layers. We then ask: (i) What would be the mean rate of energy dissipation in those boundary layers (averaged over one complete cycle), if the fluid motion deep in the interior consisted of only one of the modes described by equations (3)–(5), and if the sphere itself oscillated either in accordance with equation (1) or else not at all? (ii) In the same circumstances, at what average rate would energy be transmitted to the fluid from its container via the viscous surface stresses combined with the unsteady rotation? The first question is plainly related to the rate of free decay of the particular mode; both are involved in the balance between the mean energy input and dissipation which must by definition be struck during steady resonance.

In principle, these two questions are readily answered to leading order in both the Ekman number,

$$E = \nu/\omega a^2, \tag{6}$$

and the Rossby number or the angular half-amplitude, ϵ, by forming appropriate averages over the oscillatory Ekman layer, first with regard to depth and time at any given locality, and then over the entire spherical boundary. The actual computation is cumbersome. But if we write $M = \mathrm{Re}(A_{nm})$ and $N = \mathrm{Im}(A_{nm})$ for short, the time-averaged dissipation over the entire boundary layer works out eventually as

$$D_{\mathrm{bl}} = \rho\epsilon^2\omega_{nm}^2 a^4 (\omega_{nm}\nu)^{\frac{1}{2}}[\kappa^2 I_0 + 2\kappa I_1 M + I_2(M^2+N^2)], \tag{7}$$

where $\kappa = 1$ if the sphere itself oscillates, and $\kappa = 0$ if it does not, ρ is the fluid density, and

$$I_q = 2^{-\frac{3}{2}}\pi(x_{nm})^{-q-\frac{1}{2}} \int_{\theta=0}^{\pi} \sin^3\theta \left[\frac{U(\sin\theta, \cos\theta)}{\sin\theta\cos\theta}\right]^q \tag{8}$$

$$[\,|\cos\theta + x_{nm}|^{\frac{1}{2}}(\cos\theta - x_{nm})^q + |\cos\theta - x_{nm}|^{\frac{1}{2}}(\cos\theta + x_{nm})^q]\,d\theta$$

for $q = 0$, 1 and 2. Here θ denotes the co-latitude on the sphere and the function U is that defined in (4). Likewise, the mean rate of input P of mechanical energy, defined as the time-averaged surface integral of the product of the ϕ-component of the shear stress at the interface and the excess motion $\kappa\epsilon a\omega \sin\theta\cos\omega t$ of the container, may be determined as

$$P = \rho\epsilon^2\omega_{nm}^2 a^4 (\omega_{nm}\nu)^{\frac{1}{2}}[\kappa^2 I_0 + \kappa(I_1 M - I_{1s} N)], \tag{9}$$

Mode									$\pm (C_p)_{\max}$	
n	m	x_{nm}	I_1 equation (8)	I_{1s} (9)	I_2 (8)	I_{2s} (14)	I_e (12)	I_d (17)	$z = 0$	$z = \frac{1}{2}a$
1	1	0·6547	−0·761	−0·092	2·203	−0·278	0·745	31·3	+0·174	+0·098
2	1	0·4688	0·631	0·032	1·453	−0·100	0·303	47·3	−0·194	−0·103
2	2	0·8302	0·214	0·031	1·023	−0·163	0·379	59·1	+0·005	+0·034
3	1	0·3631	−0·550	−0·016	1·262	−0·057	0·192	71·9	+0·187	+0·097
3	2	0·6772	−0·192	−0·013	0·466	−0·045	0·112	41·9	−0·004	−0·054
3	3	0·8998	−0·097	−0·015	0·783	−0·136	0·299	111·8	+0·011	+0·003
4	1	0·2958	0·494	0·009	1·184	−0·039	0·142	103·8	−0·176	−0·090
4	2	0·5652	0·174	0·007	0·334	−0·023	0·061	44·1	+0·003	+0·063
4	3	0·7845	0·092	0·007	0·291	−0·033	0·074	53·7	−0·021	−0·007
4	4	0·9340	0·054	0·008	0·690	−0·125	0·268	194·8	+0·001	+0·021

TABLE 1. Some theoretical properties of the modes.

where I_{1s} denotes an integral that differs from the above I_1 only by the radicals $|\cos\theta \pm x_{nm}|^{\frac{1}{2}}$ having been replaced by $\pm \operatorname{sgn}(\cos\theta \pm x_{nm})\,|\cos\theta \pm x_{nm}|^{\frac{1}{2}}$, respectively. Numerical values of the integrals I_1, I_{1s} and I_2 for all ten modes of figure 1 are reported in table 1. Also recorded there for later reference are values of another integral I_{2s}, which is related to I_2 in exactly the same way as I_{1s} is related to I_1.

From the necessity that $D_{\mathrm{bl}} = P$ during the steady forced oscillation of the fluid (supposedly in a single n, m mode at or near the resonant frequency ω_{nm}), it follows at once that

$$(2I_2M + I_1)^2 + (2I_2N + I_{1s})^2 = I_1^2 + I_{1s}^2. \tag{10}$$

Thus the two components M, N of the energetically possible steady-state response amplitude of the fluid must lie on a circle in the complex amplitude plane. This circle passes through the origin $M = N = 0$, and its diameter, and hence also the maximum admissible $|A_{nm}|$, is independent of the viscosity.

Energy considerations lead also to the following simple estimate of the time t_{nm} required for the e-fold free decay of the amplitude of the (n, m)th mode due to a slight viscosity. We note that the corresponding inviscid mode has at any instant the kinetic energy

$$\text{K.E.} = \tfrac{1}{2}\rho c^2 \omega_{nm}^2 a^5 (M^2 + N^2) I_e, \tag{11}$$

where

$$I_e = 4\pi \int_{R=0}^{1} \int_{Z=0}^{(1-R^2)^{\frac{1}{2}}} (U^2 + W^2)\, R\, dZ\, dR. \tag{12}$$

Hence in the absence of excitation, or when $\kappa = 0$,

$$t_{nm} = 2\,\text{K.E.}/D_{\mathrm{bl}} = E^{-\frac{1}{2}}(I_e/I_2)\,\omega_{nm}^{-1}, \tag{13}$$

where the Ekman number E now refers specifically to $\omega = \omega_{nm}$. Some values of the integral I_e are also recorded in table 1.

As we said earlier, these results are noteworthy not for their rigor but merely the ease with which they reproduce, and hence elucidate, parts of Greenspan's analyses. For instance, despite differences of notation (which, together with Greenspan's use of disturbance pressure rather than a stream function, make detailed comparisons too lengthy to describe here), the reciprocal of our t_{nm} can be shown to be entirely equivalent to the real part of the dimensionless damping rate s_{nk1} described in Greenspan (1964, equation (4.14)). Thus the explicit integral in his equation must likewise refer to dissipation, and N_{nk} there is in essence the energy content of the mode.

Our response circle of (10) is also borne out by Greenspan's study of the forced oscillations of the fluid. That expected amplitude, derived in principle already in §6 of Greenspan (1964), is more conveniently given in equation (2.14.8) of Greenspan (1968). If we assume, for simplicity, that $|(\omega/\Omega) - 2x_{nm}| \ll 1$, and ignore all terms of that order, that equation states in effect that

$$M + iN \cong -\frac{I_1 + iI_{1s}}{I_2 + iI_{2s} + iE^{-\frac{1}{2}} I_e (\omega - \omega_{nm})/\omega_{nm}}. \tag{14}$$

From this, (10) follows immediately.

On the other hand, several aspects of the fluid behaviour clearly cannot be deduced from energy considerations alone. One of these is the indication in (14) that the greatest modal response occurs at a value of the excitation frequency ω which exceeds the inviscid ω_{nm} by the amount

$$(\delta\omega)_{nm} = E^{\frac{1}{2}}(-I_{2s}/I_e)\,\omega_{nm}, \tag{15}$$

or by a fraction $\frac{1}{2}(-I_{2s}/I_2)$ of the frequency interval between the expected half-power (or $\pm 45°$ phase) points of the response peak. This shift of the resonant frequency due to viscosity is also implied by the imaginary part of Greenspan's (1964) s_{nk1}. (Either version can be interpreted as reflecting the latitude dependence of the $O(E^{\frac{1}{2}})$ displacement thickness of the Ekman layer. Because of this, the essentially inviscid interior fluid oscillates in what appears to be a slightly

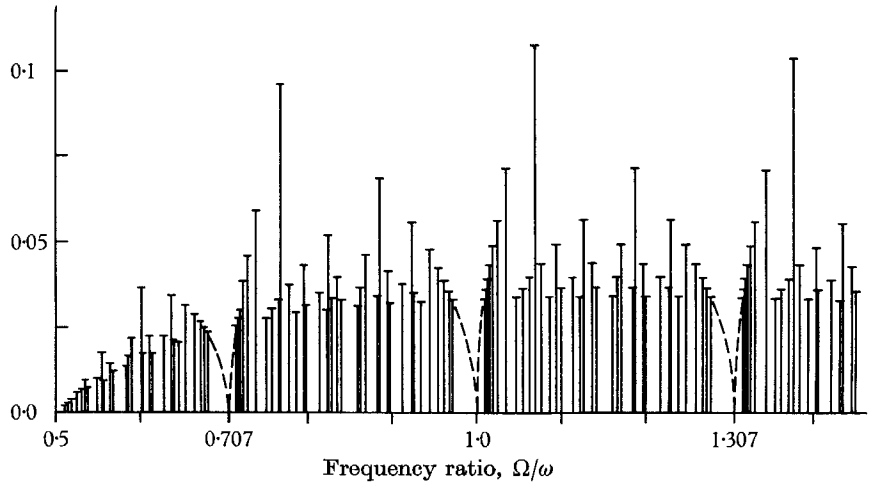

FIGURE 2. Theoretical velocity response amplitudes in the limit $\nu \to 0$.

dented container.) Energy arguments alone would also not have revealed the detailed ω dependence of $M + iN$ shown in equation (14), nor would they have provided the assurance that various modal responses can be superposed linearly. Admittedly, those last two facts could have been surmised by analogy with a mechanical system of masses and linear springs driven *through* a viscous dashpot. But such an expedient no longer seems called for.

The maximum theoretical pressure difference *amplitudes* $|\Delta p|$ between the pole and the centre ($z = 0$) of the sphere and between the pole and the point $z = \frac{1}{2}a$ on the axis are summarized in table 1. They are there recorded in terms of the dimensionless pressure coefficients

$$C_p = |\Delta p|/(\rho\epsilon\omega^2 a^2), \tag{16}$$

which will also shortly serve to describe the data. To convey a rough idea of the phase of the fluid oscillation near any given resonance, a + sign in front of an entry means that the greatest overpressure at the interior point occurs at approximately that instant when the sphere itself spins most rapidly. A − sign denotes the opposite. In addition, the arrowheads in figure 1 have all been drawn

to correspond to the expected resonant motions at an instant when the container experiences its greatest angular deceleration.

An almost alarming view of the theoretical complexity of the fluid response in the $\nu \to 0$ limit where all resonances become arbitrarily narrow is provided by figure 2. Shown there as multiples of $\epsilon\omega a$ are the expected (vertically and time averaged) root-mean-square speeds u_z along the $r = 0$ axis for various members of the $(n,1)$, $(n,2), \ldots, (n,8)$ series of modes. Among other things, such a diagram cautions that the decline of the resonant velocity amplitudes with increasing modal complexity is not especially rapid. Also, it reveals at a glance something about the distribution of the zeroes of the Legendre functions. Although eventually dense everywhere, the reciprocal eigen-frequencies Ω/ω_{nm} through any finite m show pronounced gaps, notably near $[2\sin(\pi/N)]^{-1}$, where $N = 4, 6, 8, \ldots$. But it is perhaps reassuring that the Ekman number would have had to be some five orders of magnitude smaller than in our experiment, and the linear dimensions of any plausible apparatus maybe 100 times greater, to resolve all the detail shown in figure 2!

4. Experimental results

The observed response spectrum in figure 3 is almost self-explanatory. It consists of the pressure coefficients C_p (cf. (16)) measured between the centre and the pole of the sphere for various frequency ratios Ω/ω, whilst that container oscillated steadily with a half-amplitude $\epsilon = 8{\cdot}0°$. To be exact, each data point represents the mean of about ten crest-to-trough amplitude measurements made with calipers from the chart recording of any given run. This averaging circumvented the observed fluctuation of the order of 5% in the successive wave heights (much of which, we suspect, was due to electrical noise in the transducer setup at these low pressures of operation). As remarked already in § 2, it was the turntable speed Ω and not the oscillation rate ω that was altered from one run to the next. Thus the abscissa $\Omega/\omega = 0{\cdot}5$, below which practically no fluid response was detected, is more easily recognized as the theoretical high-frequency limit $\omega = 2\Omega$ for inertial oscillations. On the other hand, the right-hand extreme, $\Omega = 2\omega$, coincides merely with the approximate top speed of our turntable. The solid theoretical curve will for the moment remain unexplained.

Phase data to accompany figure 3 is reported in figure 4. The phase $\alpha = 0°$ has there been defined to mean that the excess pressure at the centre of the sphere attained a maximum exactly when the container itself was rotating fastest. A lag angle $\alpha = 90°$ means that the central pressure maximum occurred one quarter-cycle after the peak container speed, and so forth. The phase was actually determined by superposing a transparent reference sinusoid on the chart-recorded wave-form and sliding it in the time-like direction until the best overall fit had been found by eye. Only in the case indicated by the filled circle at $\Omega/\omega = 1{\cdot}53$ did an overtone, presumably the (1,1) mode, distort the response wave-form enough to yield a secondary maximum or minimum. Any systematic (as opposed to random) errors in figures 3 and 4 are almost certainly less than the diameters of the data points.

The sharpest resonance peak in figure 3 would also have been the tallest had the pressure coefficient C_p been based on Ω^2 instead of ω^2. Not surprisingly, this peak and the rapid 180° phase change in figure 4 virtually coincides with the abscissa $\Omega/\omega = (2x_{11})^{-1} \cong 0{\cdot}764$ predicted for the fundamental (1,1) mode. Moreover, each of the other three pronounced peaks falls easily within 1% of the

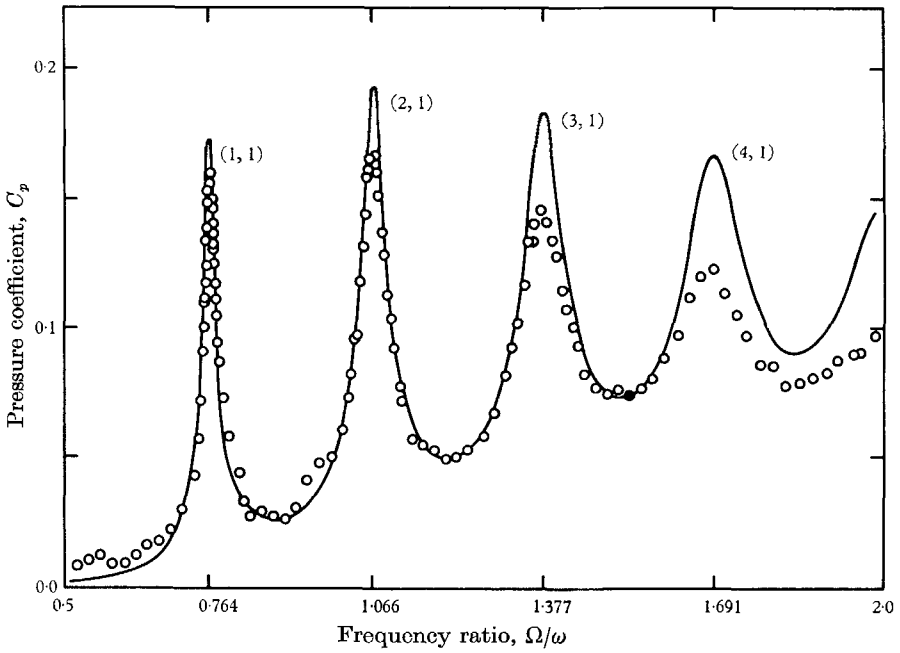

FIGURE 3. Pressure amplitudes at the centre of the sphere, for $\epsilon = 8{\cdot}0°$.

numerical values 1·066, 1·377 and 1·691 (corresponding to $(2x_{n1})^{-1}$, $n = 2$, 3 and 4). This strongly suggests that all four resonances involve successive members of the $(n,1)$ series of modes.†

That mode identification may be completed by comparing the heights of these observed peaks with the theoretical, $\nu \to 0$ resonant pressure amplitudes listed in table 1. Alternatively, one might refer to either figure 6 of Bretherton, Carrier & Longuet-Higgins (1966) or figure 2.8 of Greenspan (1968). Both those figures contain exactly the same data as the present figure 3, but they show the expected $\nu \to 0$ values of $(C_p)_{\max}$ for the $(n,1)$, $(n,3)$ and $(n,2)$ series (in order of decreasing magnitude) by means of vertical bars erected at the appropriate frequencies. Now it is true that the agreement between the observed and theoretical amplitudes leaves something to be desired. But clearly the pressure coefficients of no other modes even approach those of the $(n,1)$ series.

It should perhaps be emphasized again, however, that this predominance of

† Greenspan's prediction of the frequency shift $(\delta\omega)_{nm}/\omega_{nm}$ due to viscosity here amounts to only $1{\cdot}5 \times 10^{-3}$ even for the (1,1) mode. This is too small to be evident in either figure 3 or 4, and remains masked even on an expanded scale by finite amplitude effects and the slight non-sphericity of the container.

the $(n,1)$ coefficients does not merely stem from the decrease of the predicted velocity amplitudes of the other modes with increasing complexity (e.g. recall the 'forest' in figure 2, and compare that with the sparser tall 'trees' in the aforecited figures). Mainly, it reflects just the fact that our measurement of the centre-to-pole pressure differences discriminates against modes having more than one layer of cells in the vertical direction, and especially against those for which that number is *even*.

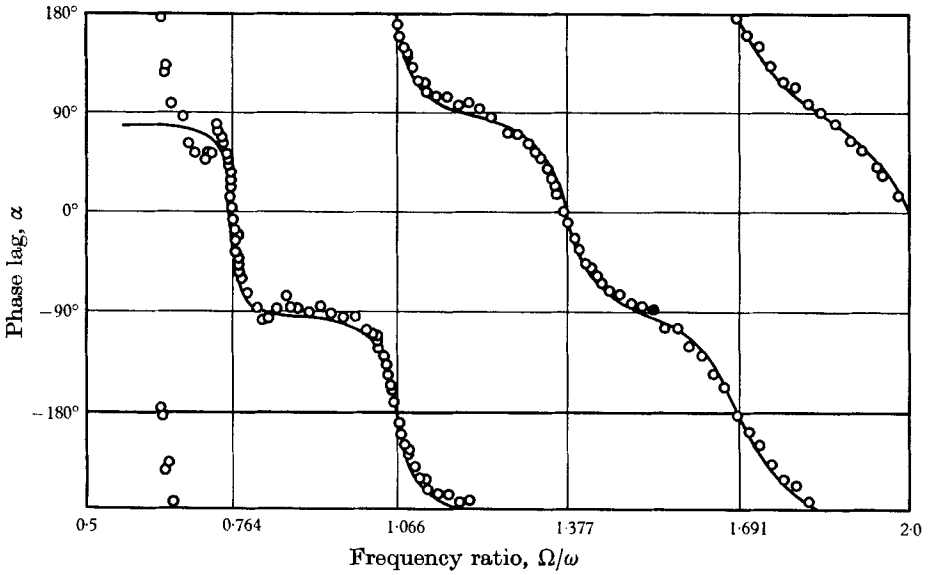

FIGURE 4. Phase of the pressure oscillations at the centre of the sphere, for $\epsilon = 8{\cdot}0°$.

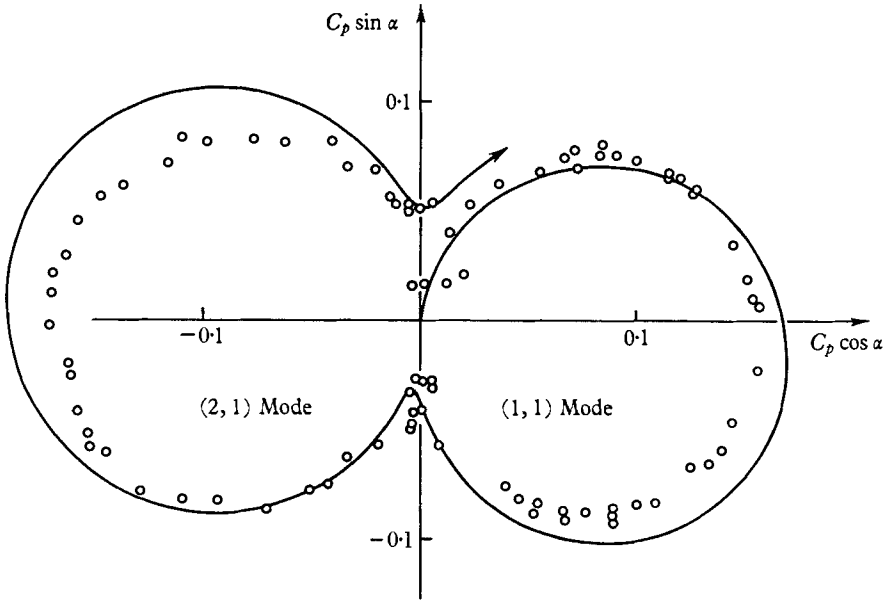

FIGURE 5. A polar plot of some of the data from figures 3 and 4.

The amplitude and phase data of figures 3 and 4 for $0{\cdot}5 < \Omega/\omega < 1{\cdot}2$ has been combined in the polar diagram of figure 5. Note that even the predicted phase *lead* $\tan^{-1}(I_{1s}/I_1) \cong 6{\cdot}9°$ for the (1,1) mode at its maximum is at least hinted in this display of the data.

The solid curves in figures 3, 4 and 5 represent linear superpositions of all theoretical $(n,1)$ modal responses through $n = 8$ (plus one-half of mode (9,1)). Each of those individual responses was taken to be broadened according to equation (14) by the small but finite viscosity, or the Ekman number

$$E \cong 1{\cdot}5 \times 10^{-5},$$

actually involved in the experiment. Strictly, of course, every conceivable mode should have been included in this vector superposition. We chose to limit ourselves to the $(n, 1)$ series only because of its preponderant amplitudes, the expectation that much of the other response would have been self-cancelling, and the inconvenience of doing anything else.

It is noteworthy that this limited superposition reproduces not only the approximate widths of the observed peaks and the general progression of phases between them, but even explains the rise in figure 3 of the 'valley' levels with increasing Ω/ω. On the other hand, the deficiencies in the observed peak amplitudes still remain, and require the following additional discussion.

At first, we were tempted to attribute those discrepancies almost wholly to the finite Rossby number of our experiment. Any second-order viscous effects, being only $O(E^{\frac{1}{2}})$ times those invoked above, seemed too small to matter. To check on this, the amplitude measurements near the (1,1) resonance peak were carefully repeated at several different excitation half-amplitudes ϵ, and the maximum experimental C_p for each ϵ was deduced from a best fit parabola through the observed pressure amplitudes at approximately ten distinct frequencies. Those results are plotted in figure 6, the vertical bars denoting probable errors due to all causes.

Figure 6 clearly reveals a significant Rossby number dependence of these maximum C_p's. (In part, that decrease with increasing ϵ must be due to boundary layer instabilities such as were in fact observed in a progressively wider band of low latitudes for $\epsilon \gtrsim 5°$.) However, this figure also shows that finite amplitude effects alone cannot fully account for the aforesaid discrepancy. Even the $\epsilon \to 0$ extrapolation for the maximum C_p falls short of the theoretical 0·174 by approximately 4%.

This difficulty was eventually resolved by an explicit computation of the time-averaged rate of viscous dissipation,

$$D_{\text{int}} = \mu\epsilon^3\omega_{nm}^2 a^3(M^2+N^2)\, I_d, \tag{17}$$

throughout the 'interior' of the fluid, i.e. excluding only the boundary layer For that purpose, the entire fluid was presumed to oscillate in a pure (n,m) mode described by equations (3) to (5). Values of I_d so obtained may be seen in table 1.

Compared to the dissipation D_{bl} in the boundary layer itself, with $\kappa = 0$ in equation (7) for simplicity, this interior dissipation is indeed formally of $O(E^{\frac{1}{2}})$. But, more exactly,

$$D_{\text{int}}/D_{\text{bl}} = E^{\frac{1}{2}}(I_d/I_2). \tag{18}$$

We find from table 1 that the numerical factor $I_d/I_2 \cong 14$ already for the (1,1) mode, and increases rapidly with increasing modal complexity. The above is, of course, not the only second-order viscous effect (the others are boundary layer corrections too awkward to estimate here). But it does make an internal viscosity correction of the order of 5% for the (1,1) mode seem quite reasonable. In fact, if that correction is taken to equal the 4% deficit at $\epsilon = 0+$ extrapolated in figure 6, then the other I_d/I_2 discrepancies suggest proportionate reductions of about 9, 16 and 25% for the (2,1), (3,1) and (4,1) response peaks, respectively. Roughly such a *trend* is indeed evident in figure 3, where the finite amplitude $\epsilon = 8°$ presumably accounts for the rest of the discrepancy.

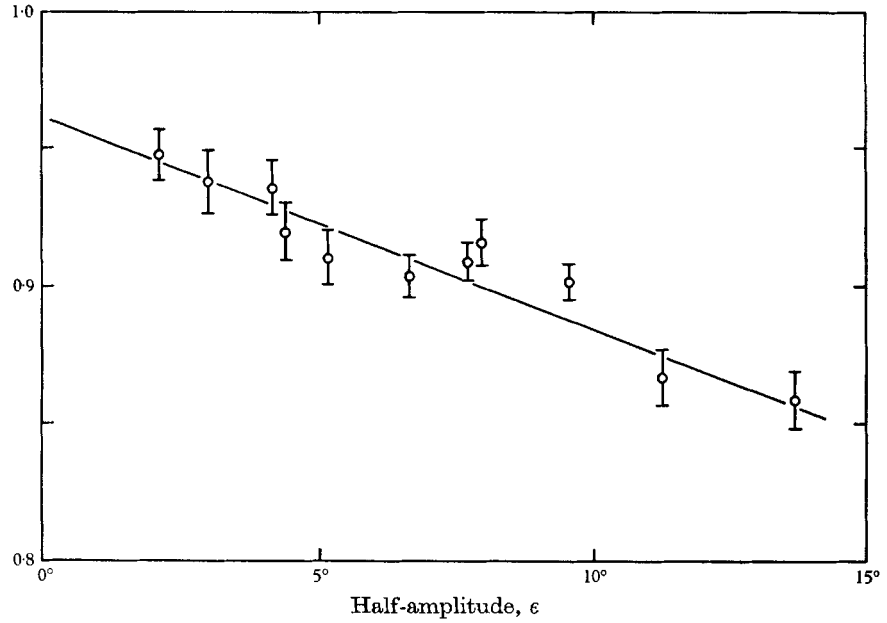

FIGURE 6. Dependence on ϵ of the heights of the (1,1) resonance peak, measured at the centre of the sphere. Shown here are the observed maximum pressure coefficients expressed as multiples of the theoretical $(C_p)_{max} \simeq 0{\cdot}174$.

Until now, our discussion of the experimental results has dwelt on centre-to-pole pressure differences. As implied before, such measurements were almost 'blind' to the $(n,2)$ mode series, for instance, owing to the expected near cancellation there of the net disturbance pressures across the two vertical cells. To detect modes of that type, we undertook some additional measurements with the probe tip immersed only half-way from the pole to the sphere centre. The amplitudes so obtained are shown in figure 7, together with $\epsilon \to 0$ and $\nu \to 0$ theoretical amplitudes shown by bars similar to those in our older version of figure 3.

Quite evident in figure 7 are new response peaks corresponding to the (2,2) and (4,2) modes. The (3,2) mode is less apparent due to its blending with the (1,1) mode; however, even on this scale, it can be detected from the broadening

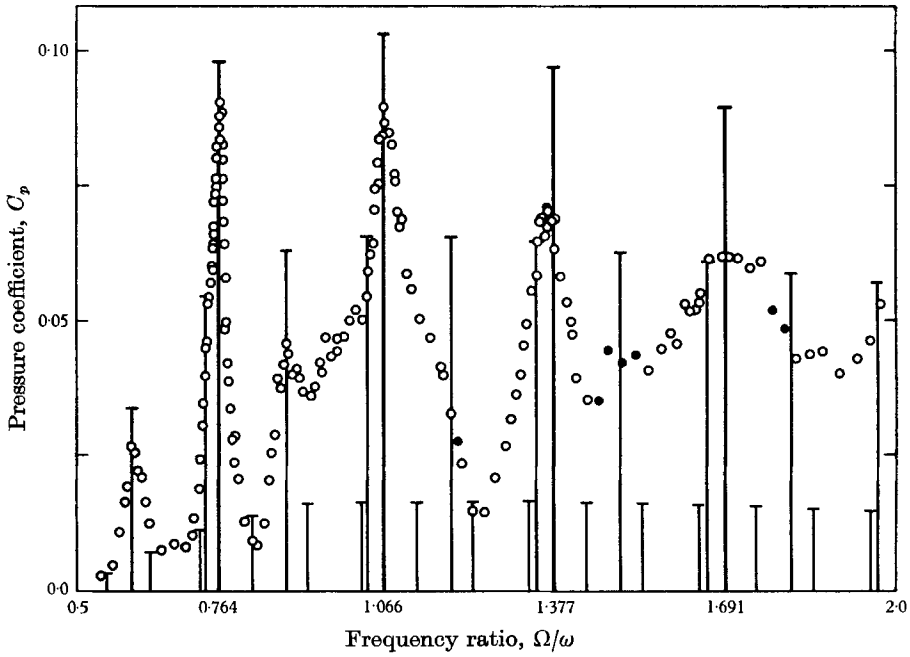

FIGURE 7. Pressure amplitudes at the half-way point $r = 0$, $z = \frac{1}{2}a$, for $\epsilon = 8{\cdot}0°$.

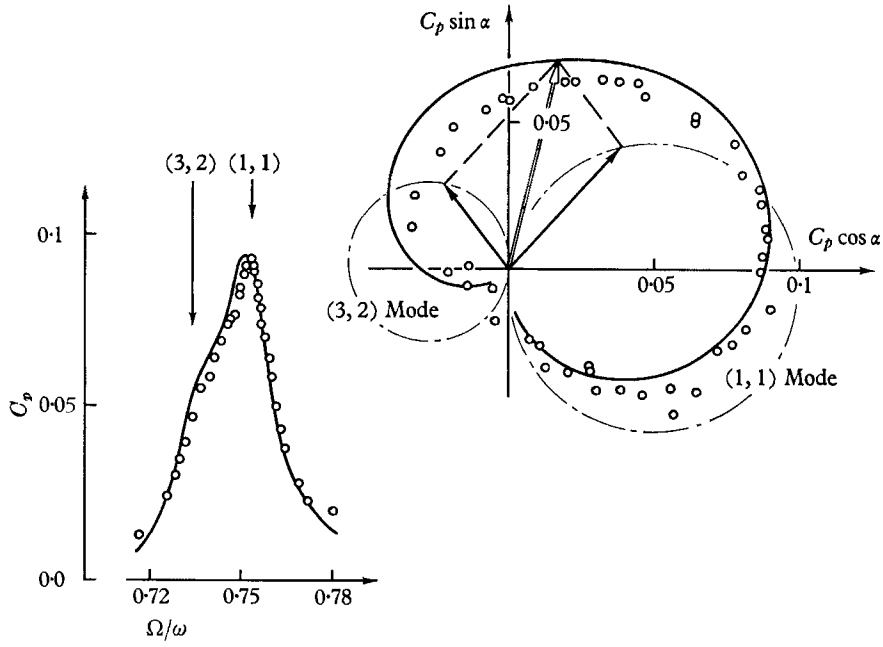

FIGURE 8. Fine structure of the (1,1) + (3,2) resonance peak, for the same conditions as figure 7.

of the first major peak as compared with figure 3. That superposition of the (1,1) and (3,2) modes is displayed in more detail in figure 8. Were the theoretical peak amplitude of the (1,1) mode reduced by about 10%, and that of the (3,2) mode by 30 or 35 (conforming with the preceding Rossby number and internal dissipation discussions), the solid theoretical curves in both parts of this diagram would indeed come into excellent agreement with the data. If nothing else, this again corroborates the view that individual modal responses can be superposed linearly.

Also recorded with our apparatus was the decay of the fluid vibrations (or, more precisely, of the centre-to-pole disturbance pressure differences) following a sudden stoppage of the oscillation, but not of the mean rotation, of the container. Prior to each run, the turntable speed Ω was fixed at a value corresponding to either the (1,1), (2,1) or (3,1) resonance peak, and the sphere itself was shaken long enough with half-amplitude $\epsilon = 8{\cdot}0°$ to establish what amounted to a steady state. Naturally, the successive peak-to-peak wave amplitudes recorded during any single decay declined roughly like $\exp(-t/T_{nm})$, with the time T_{nm} depending on the mode. Those observed mean damping times are reported in dimensionless form in table 2. Also given there are their theoretical counterparts I_e/I_2 from (13) and table 1.

Mode			
n	m	$E^{\frac{1}{2}}\omega T_{nm}$	I_e/I_2
1	1	$0{\cdot}31_5$	0·338
2	1	0·20	0·209
3	1	0·13	0·152

TABLE 2. Observed and theoretical damping times.

It is hardly surprising that the actual decays proved more rapid than those predicted theoretically. We have already remarked on the not quite negligible internal dissipation. Some additional energy loss at the higher amplitudes must also have resulted from mild roll instabilities of the oscillatory boundary layer, as observed near the equator especially during free decay.

Quite unexpectedly, however, nearly every decay record was also found to be complicated by a quasi-periodic amplitude modulation. Depending on the resonance, this modulation amounted to some 10–30% of the instantaneous amplitude and involved periods of about 3–5 oscillation cycles. From some analogous multiple-mass-and-spring systems subsequently studied numerically, we conclude that this beating was probably due to the combined action of *several* viscous modes with frequencies x_{nm} not too far from the primary. To slight extent, all those modes must have responded at the driving frequency to the steady oscillation of the container. They apparently reverted to their own natural frequencies, and hence drifted out of synchronism whilst decaying, only when the forcing was halted.

Even with that complication, though, the 'quality factor' $Q = 40{\cdot}3 \pm$ about 1·0 here implied by the mean decay rate of the (1,1) mode, and defined as usual

as the reciprocal of the fractional energy loss per radian period, agrees tolerably well with $Q \cong 42{\cdot}5$ deduced from the amplitude half-width and with $Q \cong 44$ given by the $\pm 45°$ relative phase points.

A complementary experiment, in which the sphere suddenly began to oscillate after a previously uneventful rotation, offered nothing new except at rather large amplitudes, at which an interesting overshooting was observed. That behaviour for $\epsilon = 20°$ is illustrated in figure 9 by the pressure time histories recorded for

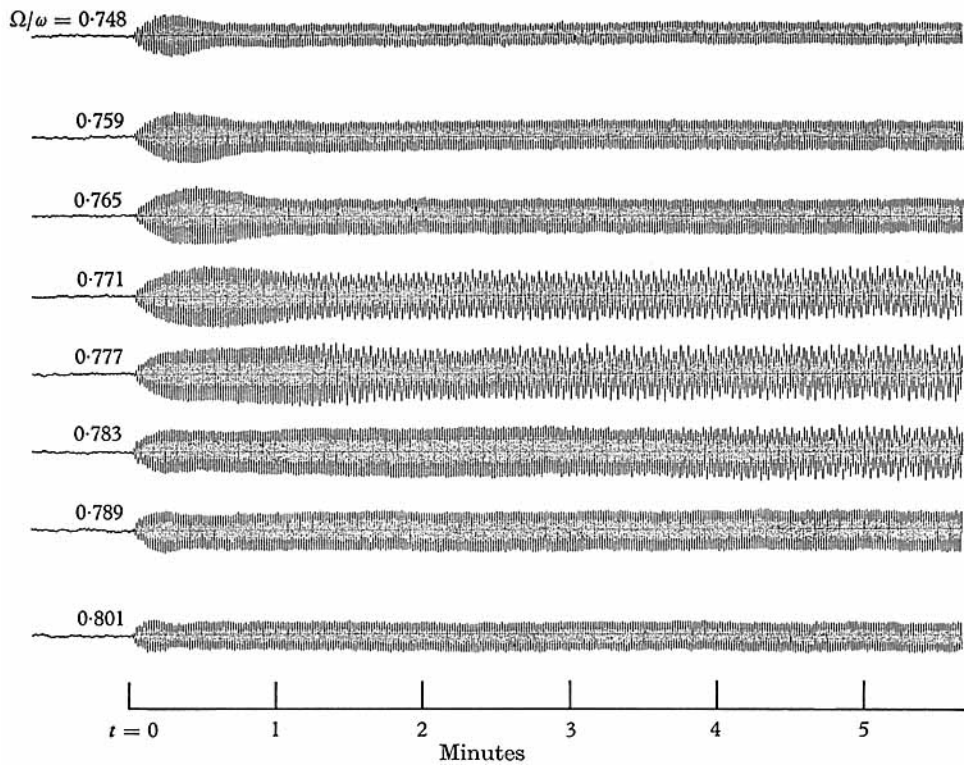

FIGURE 9. Some histories of the centre-to-pole pressure differences. The sphere started to oscillate at $t = 0$.

several Ω/ω in the vicinity of the (1,1) resonance. The greatest transient amplitudes shown there fall only slightly below the extrapolation to 20° of the straight line in figure 6. The slow adjustment in figure 9 towards the eventual response amplitudes in figure 9 seems to reflect the observed gradual establishment of a retrograde zonal flow. The middle records become curiously irregular after that adjustment; for this, we will not even attempt an explanation.

Finally, in a related series of experiments, a concentric sphere (of outer radius equal to either 2·5, 3·5 or 5·0 cm) was fastened from beneath to an axial post within our basic spherical container. For the fluid in such spherical shells, spectra analogous to those of figures 3 and 7 were obtained, and are reported elsewhere (Aldridge 1967). The resonant frequencies, so observed for counterparts of the (1,1), (2,1) and several other modes, seem in good agreement with those calculated from a certain variational principle.

We are much indebted to the patience and advice of Raymond Hide, in whose laboratory this experiment was performed. We have also benefited from discussions with Harvey Greenspan, and from the financial support (in part) of the National Science Foundation.

REFERENCES

ALDRIDGE, K. D. 1967 Ph.D. Dissertation, Department of Geology and Geophysics, M.I.T.

BJERKNES, V. & SOLBERG, H. 1929 *Avhandl Norsk Vid. Akad. Mat. Nat. kl.* **7**, 1.

BRETHERTON, F. P., CARRIER, G. F. & LONGUET-HIGGINS, M. S. 1966 *J. Fluid Mech.* **26**, 393.

FULTZ, D. 1959 *J. Meteorol.* **16**, 199.

GREENSPAN, H. P. 1964 *J. Fluid Mech.* **21**, 673.

GREENSPAN, H. P. 1968 *The Theory of Rotating Fluids*. Cambridge University Press.

KELVIN, LORD 1880 *Phil. Mag.* **10**, 155.

STEWARTSON, K. & ROBERTS, P. H. 1963 *J. Fluid Mech.* **17**, 1.